Nanofluid convection taking into account the Soret effect and its impact on heat transfer and fluid flow

Ibtissem Mhamdi[1,*], *Fakhreddine S*. Oueslati[2,*] *Rachid* Bennacer[3]

[1]Université de Tunis El Manar, Faculté des sciences de Tunis (FST), LETTM, TUNISIA
[2]Université de Carthage, Ecole Nationale d'Ingénieurs de Carthage (ENICarthage), TUNISIA
[3]LMT/ENS-Cachan/CNRS/Université Paris Saclay, 61 av. Du Président Wilson, 94235 Cachan, France

Abstract. The present study is a numerical simulation of natural convection in nanofluids, within in a square cavity differentially heated, to identify the fluid flow and heat transfer by considering the Soret effect during which a temperature gradient in a binary mixture gives rise to a concentration gradient. The governing equations solved numerically using the finite element method following the use of COMSOL Multiphysics. The effects of various parameters, the Rayleigh number, the nanoparticle concentration and the type of nanofluid are analyzed. Our simulations reveal that the heterogeneity of the nanofluid, which is generated by the Soret effect, increases the heat transfer.

1 Introduction

The progression of heat transfer by convection is the main object of several works that is why a large number of researchers have conducted a multitude of numerical and experimental tests on the description of phenomena managing convection. In this sense, the study by Oueslati and al. [1] found an analytical and numerical solution to the convection problem in a shallow cavity filled with two immiscible superimposed fluids. Bin Yuan and al. [2] carried out a comprehensive study to evaluate and optimize the efficiency of nanofluids both to prevent fines migration and to improve oil recovery using different approaches to use: Co-injection of nanofluids and pre-rinsing. The results obtained made it possible to extend the applications of nanofluids in reservoirs suffering from fine migration problems. They showed that Al_2O_3 nanoparticles are the best type of nanoparticles to reduce the migration of fines with greater fines fixation and deformation rates, and the delayed breakthrough of injected fines. In addition to the usual diffusion, cross-diffusion between the two agents discovered in 1856. This phenomenon called pure thermodiffusion, which experimentally demonstrated by Ludwig for gases. Soret showed, in 1879, that a similar phenomenon manifested for liquids called the Soret effect [3]. In recent studies, the problem of double thermodiffusion effects that occur under natural convection in fluid or porous media has been studied; see for example Bennacer and al. [4] Fakhreddine et al. [5] have made a competition between the driven lid and the natural convection of the nanofluids taking into account the Soret effect. They developed an analytical model and a numerical solution for natural convection in a two-dimensional vertical-cavity filled with a nanofluid heated from below and laterally. They explored the Soret effect. All results are obtained with an aspect ratio of A> 4, Pr = 6.2, and Le = 3. They concluded that natural convection caused by the lid causes an increase in heat transfer. Olfa and al. [6] conducted a numerical study using the finite volume method of natural convection heat and mass transfers during the evaporation of water in a vertical corrugated channel. This channel heated asymmetrically (or symmetrically) with a uniform heat flux density. The effects of heat flow density, relative humidity, and protrusion size analyzed. The fluid used is air, with Prandtl Pr = 0.71. The aspect ratio of the channel was kept constant (L / b = 10). The results that are obtained for temperature and humidity at the inlet of T = 298 K and Hr = 30% show the influence of the surface protrusion surface heat flux density, on the heat and mass transfers, the numbers of Nusselt and Sherwood. Eyuphan Manay and al. [7] conducted an experiment on the effects of the presence of TiO_2 nanoparticles in the base fluid (water) on the entropy generation rate in a micro-channel heat sink. The cases of H = 500 μm and Re<450 were found thermodynamically advantageous. Mendu and al [8] have analyzed the effects of variable viscosity and variable thermal conductivity on improving heat and mass transfer in the vicinity of a wedge surface embedded in a Brinkman-Darcy flux composed of nanofluids (Au) and (Ag). The surface of the hold maintained with variable temperature and wall concentration. The system of ordinary differential equations is solved numerically using the Matlab function bvp4c using the spectral quasi-linearization (SQLM) method. The heat and mass

* Corresponding author: Fakhreddine.Oueslati@fst.rnu.tn

transfer rates depreciate for the increasing values of the fractional volume fraction as well as for the increasing values of the Darcy parameter. The main purpose of the present paper is to develop a numerical model to solve a natural convection problem in a cavity filled with nanofluids heated laterally. The main objective is to simulate the increase in heat transfer in the most realistic way, taking into account the variation of thermal conductivity and viscosity in the governing equations of the problem. So, we take into account the Soret effect, which stimulates the heterogeneity of the concentration and this by the cross effect between the temperature and concentration gradients. Thus, the modeling reflects well the dynamic and thermal interactions of the lower convective layer of the solar basins, where one can store heat.

2 Mathematical modeling

2.1 Physical problem

In this study, we are interested in a natural convection flow of a nanofluid in a square cavity in the presence of the Soret effect. The diagram of the physical problem and the coordinate system considered in this paper illustrated in Figure 1. The square cavity is filled with nanofluids: Al_2O_3-water, Cu-water, TiO_2-water, Ag-water. Each nanoparticle characterized by its thermophysical properties as shown in Table 1. The walls of the cavity are brought to two constant temperatures with $T_2 < T_1$ and the other walls are adiabatic. (fig. 1)

Table 1. Thermophysical properties of nanoparticles

	$\rho(Kg.m^{-3})$	$\beta(K^{-1})$	$K(W.m^{-1}.K^{-1})$	$C_p(J.Kg.^{-1}.K^{-1})$
Eau pure	997.1	21×10^{-5}	0.613	4179
Argent (Ag)	10.500	1.89×10^{-5}	429	235
Cuivre (Cu)	8933	1.67×10^{-5}	401	385
Alumine (Al_2O_3)	3970	0.85×10^{-5}	40	765
Titanium ($Ti0_2$)	4250	0.9×10^{-5}	8.9538	686.2

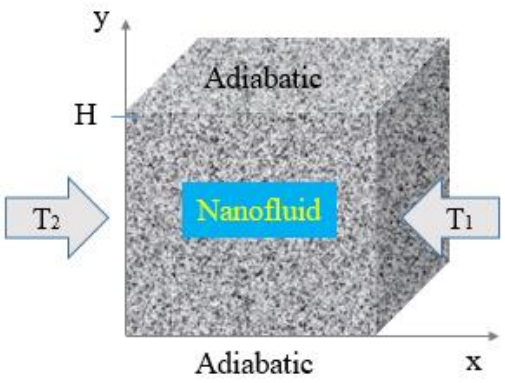

Fig. 1. Physical model and coordinate system

The nanofluid is supposed to be incompressible, the flow is laminar and two-dimensional. We assume that the nanoparticles are well dispersed in the base fluid and that they are in a state of thermal equilibrium with the base fluid. The effective thermophysical properties of the nanofluid will be approximated by different relationships from the literature. The basic fluid used is a Newtonian fluid and satisfies Boussinesq's hypothesis:

$$\rho = \rho_0\left(1-\beta_T\left(T-T_0\right)-\beta_S\left(C-C_0\right)\right)$$

Concerning the effective nanofluid properties, they evaluated using the following classical relations already known for a two-phase mixture. The effective density and specific heat of the nanofluid can be estimated following the physical principle of the mixture rule as [9] :

$$\rho_{nf} = (1-\varphi)\rho_f + \varphi\rho_p \quad (1)$$

$$(\rho C_p)_{nf} = (1-\varphi)(\rho C_p)_f + \varphi(\rho C_p)_p \quad (2)$$

Where ρ_f and φ are the density of the base fluid and volume fraction of nanoparticles respectively.
The effective dynamic viscosity of a fluid of viscosity μ_f containing a dilute suspension of small rigid spherical particles is given by Brinkman's formula [10]:

$$\mu_{nf} = \frac{\mu_f}{(1-\varphi)^{2.5}} \quad (3)$$

The thermal expansion coefficient of the nanofluid can be obtained by:

$$(\rho\beta)_{nf} = (1-\varphi)(\rho\beta)_f + \varphi(\rho\beta)_p \quad (4)$$

The thermal diffusivity of the nanofluids evaluated from:

$$\alpha_{nf} = \frac{\lambda_{nf}}{(\rho C_p)_{nf}} \quad (5)$$

The effective thermal conductivity of the nanofluid is determined according to Maxwell's model [11]:

$$\frac{\lambda_{nf}}{\lambda_f} = \frac{(\lambda_p+2\lambda_f)-2\varphi(\lambda_f-\lambda_p)}{(\lambda_p+2\lambda_f)+\varphi(\lambda_f-\lambda_p)} \quad (6)$$

The reference quantities and dimensionless variables used in this study are:

$$\left.\begin{array}{l}(x,y)=(x'/H',y'/H');\ t=t'/t^*\ ,\ t^*=H'/V^*;\\(u,v)=(u',v')/V^*\ ;V^*=U\\P^*=\rho_0.U^2\ ;\ T=(T'-T_0')/\Delta T^*;\ \Delta T'=q'H'/\lambda\end{array}\right\} \quad (7)$$

The dimensionless governing equations for, respectively, mass, momentum, energy, and species written as:

$$\nabla \vec{V} = 0 \tag{8}$$

$$\frac{\partial \vec{V}}{\partial t} + \vec{V}\nabla\vec{V} = -\nabla P + \Pr \frac{\tilde{\mu}}{\rho}\nabla^2\vec{V} + \Pr .Ra\left(T + N.C\right)\vec{k} \tag{9}$$

$$\frac{\partial T}{\partial t} + \vec{V}\Delta T = \frac{\lambda_{ea}}{\left(\rho Cp\right)_{nf}}\frac{1}{\alpha}\nabla^2 T = \tilde{\alpha}\nabla^2 T \tag{10}$$

$$\frac{\partial C}{\partial t} + \vec{V}\nabla C = \frac{1}{Le}(\nabla^2 C - \nabla^2 T) \tag{11}$$

The dimensionless parameters, that characterize the problem, are the Prandtl number $\Pr = \nu/\alpha$, the Nusselt number $Nu = hD/\lambda$, the Rayleig number $Ra = g\beta\,\Delta T H^3/\nu\alpha$, the thermal Rayleigh number $Ra_T = g\beta_T \Delta T H^3/\nu\alpha$, the solutal Rayleigh number $Ra_S = g\beta_S \Delta T H^3/\nu\alpha$, the Soret coefficient $Sr = C_0\left(1-C_0\right)\Delta C'/\Delta T'$, buoyancy rate $N = Ra_S/Ra = \beta_S \Delta C'/\beta_T \Delta T'$.

The numerical procedure used in this work based on a finite element approach. Comsol Multiphysics has been used since it is a modular finite element numerical computation software that can model a wide variety of physical phenomena characterizing a real problem.

Our results have been compared, in the case of natural convection in a square cavity, to the works of Y.L.He [12] and Bocu [13] for different Rayleigh numbers . The numerical results of these authors constitute an excellent test for the validation of our numerical code.

3 Results and discussion

3.1 Rayleigh number effect

Four nanoparticles (Cu, Ag, Al_2O_3 and TiO_2) were used. Each nanoparticle has thermophysical properties different from others. Water considered basic fluid. The nanoparticles supposedly well dispersed in the fluid and are in a state of thermal equilibrium with the latter.

Figure 2 illustrates the effect of flow intensity on the optimal value of the mass fraction for different Rayleigh numbers. From this figure, it can be seen that heat transfer is essentially conductive for low values of Ra ($Ra < 10^3$). For the high values of Ra, ($Ra \geq 10^3$), the heat transfer increases with the mass fraction of the nanoparticles up to almost ((φ = 3% for Ra = 10^3, φ = 5% for Ra = 10^4, φ = 5% for Ra = 10^5, φ = 6% for Ra = 10^6) and then decreases with increasing fraction of the nanoparticles. The overall heat transfer affected by the increase in the Ra number as well as the weight percentage of the nanoparticle. However, for each Ra, we have a critical nanofluid that gives the maximum heat transfer.

Figure 3 presents the comparison of isotherms, streamlines, and isoconcentrations using different Rayleigh numbers for Al_2O_3. For Ra = 10^2 the distribution of the isotherms in the cavity reveals a horizontal stratification reflecting a mode of transfer essentially conductive.

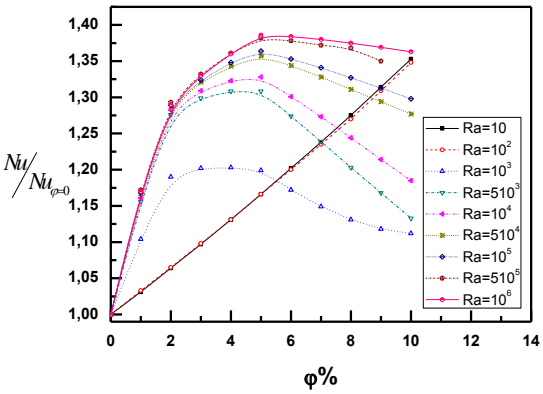

Fig. 2. Effect of nanofluid concentration on relative heat transfer for different Ra (Le=1, Sr=1,Pr=6.2)

When increasing the Rayleigh number, a clear change in stratification and temperature gradients observed highlighting the convective nature of the flow.

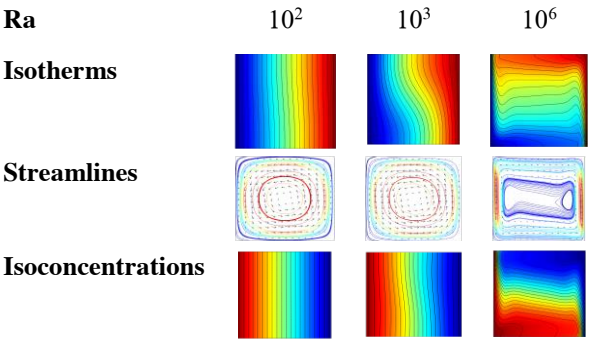

Fig. 3. Dynamic, thermal and species field for different Ra numbers for Al_2O_3

3.2 Effect of the nature of the nanoparticle

Figure 4 presents the variation of the mass fraction for different nanoparticles, one notices that the heat transfer increases monotonically with the increase of the mass fraction for all the nanofluids. For Al_2O_3 nanoparticle, there is the existence of a maximum transfer for a percentage by weight of the nanoparticles (5%) beyond which the transfer decreases significantly. In the case of Cu, which provides thermal conductivity and a density which increases remarkably with the nanoparticles: an increase of the thermal transfer quite important and the same for TiO_2. The increase in heat transfer in the different cases of nanofluids is justified by the appearance of solutal forces due to heterogeneity and which are added to the thermal forces.

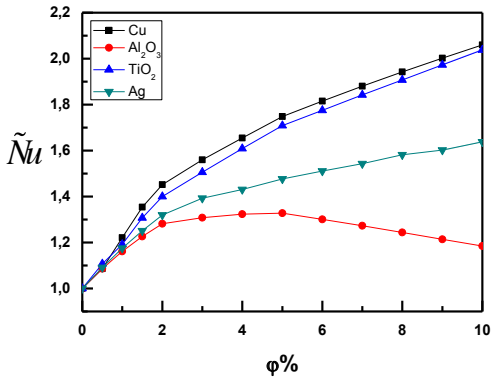

Fig. 4. Effect of nature of nanoparticle on the nanofluid heat transfer: heterogeneous case(Ra=10^4,Pr=6.2,Le=1,Sr=1)

Figure 5 shows a comparison of isotherms, streamlines, and isoconcentrations for different nanofluids for Ra = 10^4. The figure demonstrates that for all nanofluids, a single cell motion observed in the opposite direction of clockwise.

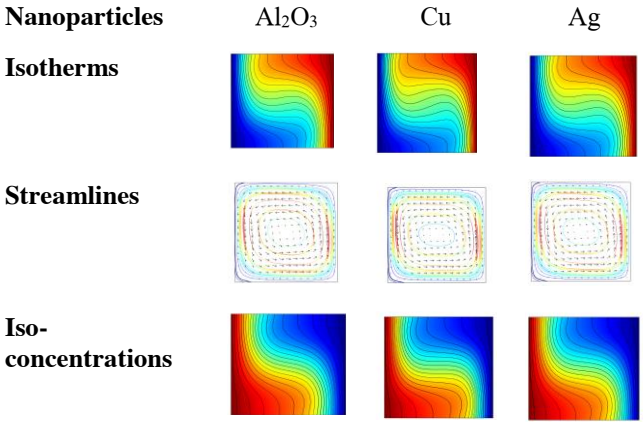

Fig. 5. Dynamic ,thermal and species fields for different type of nanoparticle(φ =6%, ,Ra=10^4,N=0.75,Le=1,Sr=1)

Isoconcentrations shows that the Soret effect affects spatial heterogeneity, which in turn leads to a change in the thermal field that can modify the rate of heat transfer. These figures show that such heterogeneity of the particle concentration induces additional buoyancy forces and modifies the momentum equilibrium. Although actually, the thermal, dynamic, and concentration fields are affected that are not very legible but by drawing the profiles of temperature, concentration, and velocity in the horizontal median plane illustrated by figure 6.

One notes that the profiles of temperatures, concentration, and speed are quite distinct and reveal a quite remarkable temperature and concentration gradients. The temperature and concentration profiles as well as the velocity profiles highlight that the streamlines and the isotherms are distinct. The velocity shows a parabolic variation near the vertical walls. Vertical velocities are sensitive to the nature of nanoparticles where they are very distinct for different nanofluids.

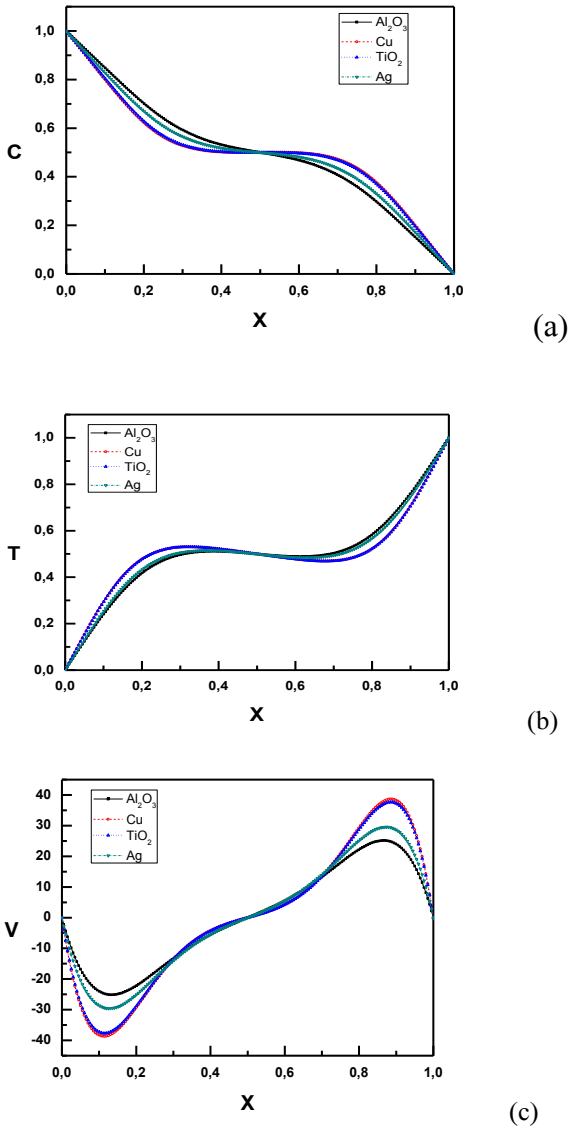

Fig. 6. Concentration (a), temperature (b) and vertical velocity (c) on the horizontal mid-plan (φ =6% , Ra=10^4, Pr=6.2, Le=1,Sr=1)

Conclusion

Numerical study of natural convection for different nanofluids in a two-dimensional square cavity. Therefore, the choice of the type of nanofluid is an important factor to maximize heat transfer. In addition, the increase in the mass fraction of nanoparticles increases heat transfer. However, in the case of nanofluid convection, the increase in the number of Rayleighs affects the increase in heat transfer. However, the highest values of heat transfer are obtained with Cu copper nanoparticles. Soret's cross effect is responsible for the spatial distribution of nanoparticle concentrations, and it influences heat transfer as well as the dynamic field.

Nomenclature:

g	Gravitational acceleration; m/s^{-2}
C_p	Heat capacity

Nu	Nusselt number
Pr	Prandtl number
Ra	Rayleigh number
x,y	Dimensional space coordinates; m
u,v	Dimensional composents of speed

Greek Symbols:

α	Fluid thermal diffusivity ; $m^2.s^{-1}$
$\beta = \frac{1}{T}$	Coefficient of volume dilation ; k^{-1}
μ	Dynamic viscosity ; $Kg.s^{-1}.m^{-1}$
ν	Kinematic viscosity ; $m^2.s^{-1}$
φ	Mass fraction ; %
ρ	Density ; $Kg.m^{-3}$
λ	Thermal conductivity ; $w.m^{-1}.k^{-1}$
λ_{eff}	Effective thermal conductivity
λ_s	Thermal conductivity of nanoparticles
λ_f	Thermal conductivity of the fluid

Subscripts

P	Particle
F	Fluid
N_f	Nanofluid
N_p	Nanoparticle

References

1. F. S. Oueslati, R. Bennacer, M. El Ganaoui Int. J. of Ther. Scien., 303-310, (2015).
2. R. Ben Yuan, M. Ghanbarnezhad, W. Wendong. Fuel, **215**, 474, (2018).
3. E. K. Vafai, Analysis of heat and mass transfer.
4. R. Bennacer, Mahidjiba A., Vasseur P., Beji H., R. Duval. Int. J. Numer. Meth. Heat Fluid Flow, **2**, 199 (2003).
5. F. S. Oueslati, R . Bennacer, M. El Gannaoui, A. El Cafsi., Inter. Jour. of Hea. and Mass Trans. **114**, 1341 (2017).
6. O. Mechergui, Xavier Chesneau . Energy. Procedea., **139**, 791 (2017).
7. Eyuphan Manay, Eda Feyza Akyurek, Bayram Sahin. Résultats en physique, 615 (2018).
8. Mendu, Upendar, Venumadhav, J. of Nanof., **8**, 230 (2019).
9. Y. Xuan, W. Roetzel Int. J. of Heat and Mass Trans. **43**, 3701 (2000).
10. H. Brinkman, J.Chem. Phys., **20** 571 (1952).
11. J. Maxwell, Oxford University Press, Cambridge, UK, pp. 435-441, (1904).
12. He, Y.L., Yang, W.W. Numer. Heat Transf. Part A, **47**, 917 (2005).
13. Z. Bocou Z., Altac, Appl. Ther. Engine. **3**, 3189 (2011).